Weather and Climate Extremes 26 (2019) 100236

Contents lists available at ScienceDirect

Weather and Climate Extremes

journal homepage: http://www.elsevier.com/locate/wace

Variability and predictability of winter cold nights in Argentina

Soledad Collazo [a,b,*], Mariana Barrucand [a,b], Matilde Rusticucci [a,b]

[a] Departamento de Ciencias de la Atmósfera y los Océanos, Facultad de Ciencias Exactas y Naturales, Universidad de Buenos Aires, (DCAO-FCEN-UBA), Argentina
[b] Consejo Nacional de Investigaciones Científicas y Técnicas, (CONICET), Argentina

ARTICLE INFO

Keywords:
Seasonal forecast
Predictability
Extreme temperature
Climate prediction
Argentina
Climate indices

ABSTRACT

Extreme cold events can cause crop damage as well as an increase in energy demand and even in the mortality rate. Identifying the atmospheric processes associated with the occurrence of these extremes would allow decision-makers to implement preventive and mitigation actions. The goal of this study is to identify predictors of cold extremes of minimum temperature during winter in Argentina (north of 40 °S), and their modulation by the different El Niño-Southern Oscillation (ENSO) phases for the period 1970–2015. Lagged correlation analysis between winter cold nights and several global and regional climate indices identified ENSO, subtropical jet intensity, position and intensity of the South Pacific Anticyclone (SPA), and a blocking index as the dominating forcings. The El Niño phase is associated with a decrease in the occurrence of cold extremes. In addition, an increase in the number of blocking events together with a weaker subtropical jet and, a less intense and northward shift of the SPA also inhibit the occurrence of cold extremes of the minimum temperature. Our results indicate persistence in the winter cold nights series compared with the previous season in eastern Argentina. Two winters with opposite extreme conditions (high and low frequency of cold nights) were selected as case studies. Since both cases occurred under ENSO neutral conditions, we also searched for cold nights predictors considering only neutral years. We detected the presence of an equivalent barotropic structure located in southeastern Pacific in both events, which confirmed the importance of the SPA intensity and blocking events as predictors in absence of an active El Niño.

1. Introduction

Cold extreme events can lead to extensive agricultural damage, and in Argentina, studies have reported a large impact to regional and national economies (Verdes et al., 2000; Müller, 2010; Barlow et al., 2015). Given their impacts it is important to understand the mechanisms that trigger those cold extreme events and improve their forecast.

Cold outbreaks and cutoff lows cause severe-weather events over southern South America during the austral winter. Major cold-air outbreaks are the result of an upper-level subtropical cyclonic perturbation associated with a further northward location of the subtropical jet stream, facilitating the equatorward penetration of frontal systems (Vera and Vigliarolo, 2000). Changes in upper-level circulation, with the jets as the most characteristic features, are related to changes in circulation at low levels. At monthly and seasonal scales, Barros et al. (2002) found that the intensification (reduction) of upper-level westerlies over southern South America tends to be associated with negative (positive) anomalies of the surface temperature. In addition, they observed that the northward (southward) displacement of the subtropical jet over southern South America also results in negative (positive) temperature anomalies.

Cold air incursions can lead to regional or generalized frosts in Argentina. Monthly, seasonal and annual composites show a stronger (weaker) than normal subtropical jet over South America associated with a higher (lower) frequency of frost occurrence (Müller et al., 2005; Müller, 2007). Müller and Berri (2012) studied the atmospheric circulation associated with extreme generalized frosts in central-southern South America, noting that the largest persistence events are associated with Rossby wave train propagation across the Pacific Ocean and with the magnitude of the confluence in the jet entrance region in subtropical latitudes.

Blocking events over the Pacific Ocean near the coast of Chile perturb atmospheric circulation over southern South America, leading to quasi-stationary mid-latitude systems for several days. Alessandro (2014) related the location of the blocking pattern with temperature change, demonstrating that blocking events located at 70 °W cause

* Corresponding author. Departamento de Ciencias de la Atmósfera y los Océanos, Facultad de Ciencias Exactas y Naturales, Universidad de Buenos Aires, Ciudad Universitaria Pab II, Buenos Aires, Postal code: 1428, Argentina.
E-mail address: scollazo@at.fcen.uba.ar (S. Collazo).

https://doi.org/10.1016/j.wace.2019.100236
Received 14 January 2019; Received in revised form 13 August 2019; Accepted 9 October 2019
Available online 13 October 2019

negative anomalies in the winter and spring in most of Argentina. In addition, blocking events force the westerlies into two branches around 120 °W: one towards the subtropics and another towards the subpolar region, resulting in modified trajectories of extratropical cyclones and associated frontal systems.

Some aspects of the influence of different ENSO phases on the frequency of cold extremes in Argentina have been already explored. Convection anomalies associated with ENSO, cause upper-level divergence anomalies that perturb the global circulation and impact seasonal and monthly climate in several regions of South America (Grimm and Tedeschi, 2009 and the references therein). Rusticucci and Vargas (2002) found that La Niña produces more homogeneous effects on the spells of temperature extremes than El Niño does, especially for cold events. The mean number of frost occurrences is lower (greater) than climatological values during El Niño (La Niña) events (Müller et al., 2000). More recently, Rusticucci et al. (2017) showed that the impact of El Niño events on extreme temperature in Argentina presents monthly differences, favoring warmer nights during winter.

One of the most transcendental climate forcings on the Southern Hemisphere is the Antarctic Oscillation (AAO), also known as the Southern Annular Mode (SAM), since it is the most important large-scale pattern of climatic variability in the extratropical region (Gong and Wang, 1999; Thompson and Wallace, 2000). The SAM appears as the main modulator of the latitude and strength of the polar front jet, influencing to a minor extent its subtropical counterpart (Gallego et al., 2005). The positive phase of the SAM causes significant warming over southern Argentina (Gillett et al., 2006). In addition, positive (negative) phases of the SAM tend to cause cooler (warmer) sea surface temperature (SST) in the high latitudes, but warmer (cooler) SST in the middle latitudes (Zheng et al., 2015), and a reduction (increase) of the activity of the cyclonic synoptic systems and thus decrease (intensify) precipitation over southeastern South America (SESA, Silvestri and Vera, 2003). In particular, SAM has already used to predict the maximum temperature extremes in southeastern Australia (Richman and Leslie, 2014).

Following a previous study for warm extreme of maximum temperature in Argentina (Collazo et al., 2019), the goal of this work is to find predictors of the occurrence of winter cold nights (hereafter labeled JJA TN10) in Argentina north of 40 °S and evaluate the potential ENSO modulation. A first analysis of JJA TN10 time series was made in order to detect trends and periodicities of the series that could give us an idea of possible predictors acting at different timescales. Among all predictors analyzed, the persistence of TN10 was especially considered by correlating winter cold nights with autumn TN10 and May TN10. Furthermore, we explored the distributions of JJA TN10 in each ENSO phase and looked for potential predictors under ENSO neutral conditions. Finally, we analyzed the atmospheric circulation for two case studies when JJA TN10 registered extremely low and high values in order to check the contribution of the predictors in rare cases.

2. Data and methodology

2.1. Extreme temperature index

Daily minimum temperatures of austral winter (June–August, JJA) for the period 1970–2015 were used. The data of 83 conventional weather stations located in Argentina north of 40°S were provided by the National Institute of Agricultural Technology (INTA, http://siga2.inta.gov.ar/#/data) and the National Meteorological Service (SMN, https://www.smn.gob.ar/). All stations have less than 10% missing data in the period analyzed.

Quality control was performed using the freely available R-Climdex software (at http://etccdi.pacificclimate.org/software.shtml, accessed in May 2015). Data with values far above or below the expected values were also checked by manual inspection, considering the information from nearby stations and temperature evolution on previous and subsequent days.

The extreme temperature index for cold nights (TN10), defined as the percentage of days with minimum temperature below the 1981–2010 10th percentile, was calculated following the guidelines established by international literature on the subject based on recommendations by Expert Team on Climate Change Detection and Indices (ETCCDI). The index was estimated on a monthly basis and from them, seasonal values were obtained.

2.2. Trends and periodicities

The analysis of trends and wavelet spectra allows us to identify the long-term variations of the series and the presence of periodicities respectively. Linear trends of TN10 in austral winter (JJA) were calculated for the 1970–2015 period, and statistically tested by using the non-parametric Mann-Kendall test (McLeod, 2011). This test is commonly employed to detect monotonic trends in series of environmental data. The null hypothesis for this test is that there is no monotonic trend in the series (Mann, 1945; Kendall, 1975). All JJA TN10 series were then detrended for subsequent analysis.

The wavelet transform is a mathematical tool to detect intermittent periodicities that involve multiple scales of variability and the periods in which they were active, by expanding the time series into a new series that depends on time and frequency (Torrence and Compo, 1998; Grinsted et al., 2004). In our study, the WaveletComp package of R (Roesch and Schmidbauer, 2014) was applied to the JJA TN10 series by using a Morlet wavelet as the mother wave, since it is widely accepted in the literature that is the most suitable for geophysical series (Foufoula Georgiou and Kumar, 1995; and references therein). In order to test the null hypothesis of "no periodicity", the statistical significance tests for wavelet power spectra consist in deriving theoretical wavelet spectra for white noise processes and using these to establish significance levels and confidence intervals. In our case, we made 100 simulations. Missing data were replaced with the climatological value. To summarized, we only show the results in eight selected stations distributed throughout the study region (Fig. 1).

2.3. Search for predictors

We considered a variety of indices, representative of different processes and mechanisms that could influence JJA surface temperature. Indices, estimated from May data, were classified into four groups: modes of climate variability, regional atmospheric circulation, Atlantic

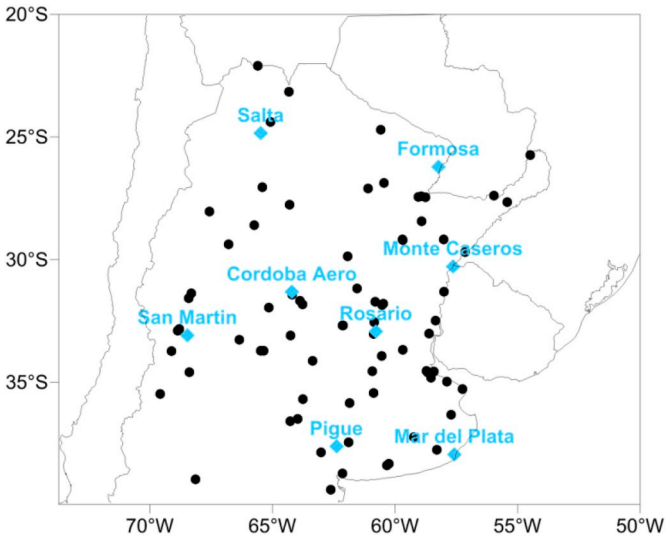

Fig. 1. Stations considered in this study, those with names were selected to display the wavelet spectrums.

SST and South American monsoon, and soil moisture conditions. We used May data in order to assess if these processes are sources of predictability of winter cold nights. The monthly atmospheric and oceanic indices were acquired from the website of the National Oceanic & Atmospheric Administration (NOAA) (http://www.esrl.noaa.gov/psd/data/climateindices/list/, accessed June 2016).

Among the climate indices, we considered El Niño1+2, Niño3, Niño3.4, Niño4, ONI, Modoki (Ashok et al., 2007), Southern Oscillation Index (SOI), SAM (Marshall, 2003), Indian Ocean Dipole (IOD, Saji et al., 1999), Tropical Southern Atlantic Index (TSA, Enfield et al., 1999), Pacific Decadal Oscillation (PDO, Zhang et al., 1997; Mantua et al., 1997), Atlantic Multidecadal Oscillation (AMO, Enfield et al., 2001).

We calculated representative indices of regional atmospheric circulation, previously proposed by other authors, using reanalysis data from the National Centers for Atmospheric Prediction (NCEP) and the National Center for Atmospheric Research (NCAR) Reanalysis 1 (Kalnay et al., 1996) because it covers the entire studied period (1970–2015). The indices capture the intensity and position of the subtropical jet (Barros et al., 2002; Rusticucci et al., 2017), blocking events (Rutllant and Aceituno, 1991; Alessandro, 2014), the intensity and position of the subtropical anticyclones in the Atlantic and Pacific Ocean (González et al., 2015), the meridional advection at lower-levels (Barros et al., 2002; Rusticucci et al., 2017).

The influence of SST in the vicinity of Argentina was represented through the indices defined by Barrucand et al. (2008) and the Atlantic dipole by Wainer et al. (2014). The Outgoing Long-Wave Radiation was used as an index of deep convective activity in tropical South America (Cerne and Vera, 2011; González et al., 2016).

The Standardized Precipitation Index (SPI) (McKee et al., 1993, 1995) was used as a proxy of soil moisture conditions (Mueller and Seneviratne, 2012). This index requires only precipitation data, which in this case was from the same stations as those used to calculate JJA TN10. We estimated the SPI for multiple timescales: 1, 3, 6, 9 and 12 months with the software available on the website http://drought.unl.edu/MonitoringTools/DownloadableSPIProgram.aspx. A missing data code was assigned to the monthly accumulated precipitation when more than 10% of data was missing. More details of the indices are in the Supporting Information.

We then calculated and tested the 1-month lagged Spearman correlations between cold nights in each meteorological station and each representative index of the different forcings mentioned above, i.e., JJA TN10 time series were correlated with the May indices. This analysis allows us to determinate the association between the forcings and JJA TN10, and to obtain information about the predictability of the series. Besides, we used 1-month lag because several climate services consider this lag to elaborate their seasonal forecast of precipitation and temperature, such as the International Research Institute or the Argentina National Meteorological Service. In order to study the persistence of the series, we also calculated and tested the correlation between JJA TN10 and May TN10 and also March–May (MAM) TN10 in the previous season.

The Spearman correlation coefficient is a measure of the nonparametric correlation between two continuous random variables that do not necessarily follow a normal distribution. To calculate it, the data is sorted and replaced by its respective order (Wilks, 2006). The statistical significance of the correlation coefficient was tested using AS 89 algorithm considering a significance level of 5% (Best and Roberts, 1975). The null hypothesis is that the two variables are not associated; the purpose of the test is to evaluate the possibility of rejecting this hypothesis. If the null hypothesis is rejected, it is concluded that there is probably an association between the variables under study. Linear trends were removed from all time-series to avoid a spurious empirical relationship.

Among all the forcings considered, we selected those who presented at least 20% of stations with significant correlations (at 95% confidence level). These forcings were called as main predictors. Then for these main predictors, the mean value of JJA TN10 was estimated for those years in which each predictor registered values above the second tercile, and for those years in which the value of the index did not exceed the first tercile. The difference between the two means was calculated, and the statistical significance was tested using a T-Student test for the mean of two samples with a significance of 95%. In addition, we applied the non-parametric Wilcoxon rank-sum test (Wilcoxon, 1945) whose null hypothesis is the equality of population medians of two independent samples. Both tests presented similar results.

Since ENSO is one of the most important sources of variability and predictability in South America (Osman and Vera, 2016), we performed a more detailed analysis of the JJA TN10 distribution for each ENSO phase. We followed the NOAA classification based on the ONI index to determine the ENSO phases (accessed in May 2016). The Kolmogorov-Smirnov test (K–S test, Smirnov 1939) was used to test if the JJA TN10 samples in each ENSO phase shared the same distribution. This non-parametric test computes the difference between the empirical cumulative distribution functions of two samples, and it is sensitive to differences in both location and shape of the empirical cumulative distribution functions of the two samples. In order to summarize the results, we clustered the stations in four groups by applying the K-means methodology (MacQueen, 1967) with the Hartigan and Wong (1979) algorithm. To perform K-means clustering, we first specified the desired number of clusters K, and then the K-means algorithm assigned each observation to exactly one of the K clusters (James et al., 2013). The idea behind K-means clustering is that a good clustering is one for which the within-cluster variation is as small as possible. The final solution is obtained by heuristic methods and might be sensitive to the initial choice for the centroids, in particular when $K > 4$. Therefore, we chose four groups to cluster the stations according to their values of JJA TN10.

Finally, we looked for predictors of JJA TN10 under ENSO neutral conditions by correlating the possible predictors and the extreme index only for these neutral years.

3. Results and discussion

3.1. Trends and wavelet analysis of JJA TN10 series

We analyzed the trends of JJA TN10 in the 1970–2015 period and their statistical significance (Fig. 2). In general terms, there is a majority of negative trends mainly in western Argentina implying a reduction in the occurrence of cold extremes of minimum temperature, in agreement with results in Chapter 2 of the Fifth Report of the Intergovernmental Panel on Climate Change working group I (IPCC, 2013). Nevertheless, also significant positive trends were found in the southeast of the study region, consistent with the monthly trends of TN10 for the 1970–2010 period presented by Rusticucci et al. (2017). All trends (significant or not) were filtered for subsequent analyses.

The main signal of the wavelet analysis indicates a 4-years period at different locations (Fig. 3), which is consistent with a previous study carried out for some reference stations in Argentina (Barrucand et al., 2008). However, this signal is not constant in the entire period; in fact, the wavelet power spectrum presents maximum values on different years according to the station considered. Some hypotheses are that this periodicity could have some influence of ENSO over extreme temperature or other global or regional mechanism or even it could be simply noise. In the following section, we analyzed the linear correlation between JJA TN10 and different forcings. A 16-year periodicity seems to be an important signal in stations located in western Argentina, suggesting the influence of low-frequency climate modes. Therefore, the PDO and AMO were incorporated as possible predictors in the analysis.

3.2. Predictors of JJA TN10

3.2.1. TN10 persistence as a predictor

We analyzed the persistence in the TN10 series by correlating May

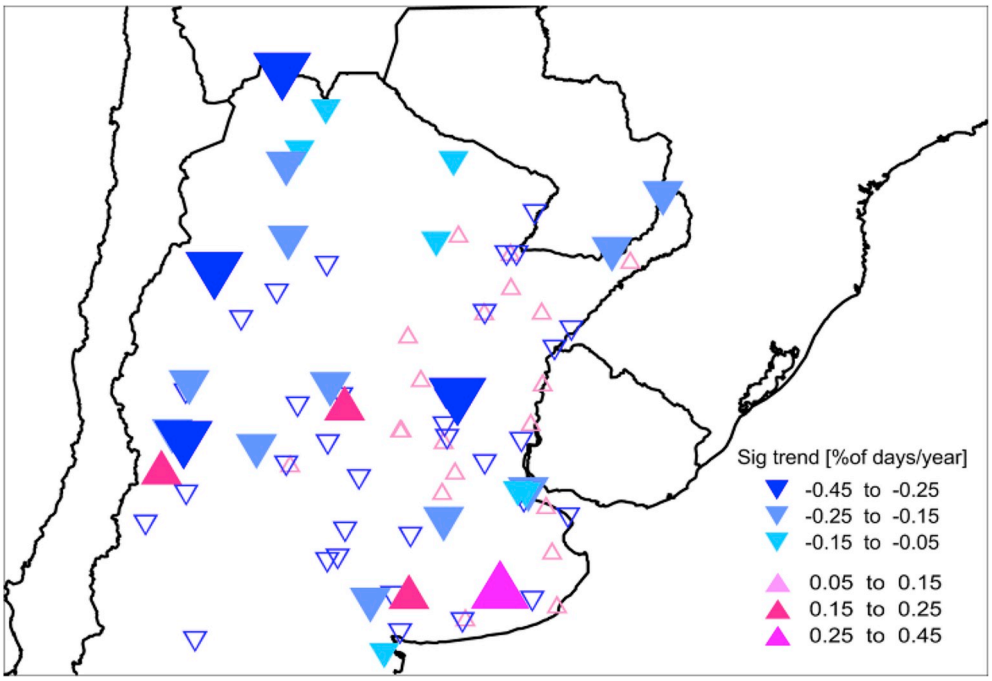

Fig. 2. Trends of JJA TN10 in the 1970–2015 period [% of days/year]. Positive significant trends are represented with solid up triangles, positive non-significant trends with small up triangles, negative non-significant trends with down triangles and negative significant trends with solid down triangles.

TN10 with JJA TN10, and MAM TN10 with JJA TN10 (Fig. 4) and found significant positive correlations only in eastern Argentina. In particular, we observed more stations significantly correlated between May TN10 and JJA TN10 than with MAM. However, the memory of the series is limited only to one particular region and not all stations; we can conclude that May TN10 could be considered a good predictor for the winter occurrence of cold nights only in eastern Argentina. The persistence of JJA TN10 could be the result of a combination of several physical features, such as fluctuations in SSTs, the annular modes, Madden-Julian oscillations, ENSO or perhaps process on longer time scales.

3.2.2. *Global climate indices*

The main modes of climate variability (ENSO, SAM, IOD, PDO, AMO), which affect the circulation of South America through teleconnections, were 1-month lagged correlated with JJA TN10. Fig. 5a presents the percentage of stations with significant correlations at 5%. The results showed that only the ENSO indices in May presented a strong association with JJA TN10 in several stations. The Niño 3 and SOI indices had the best performance with almost 30% of the stations showing significant correlations.

Fig. 6a shows the difference between mean JJA TN10 for years when May Niño 3 exceeded the second tercile, and mean JJA TN10 for years when the index was lower than the first tercile. We found significant negative differences of JJA TN10 throughout the region except in the southwest sector. These results indicate that above (below) normal anomalies of SST in the Niño 3 region during May tend to inhibit (enhance) the occurrence of cold extremes of minimum temperature during the winter. Similar results were found by Rusticucci et al. (2017) for monthly simultaneous correlations between TN10 and the ONI index, and by Loikith et al. (2017) for the percentage of extreme cold months concurrent with ENSO. In addition, Müller et al. (2000) demonstrated that the low (high) phase of SOI coincides with those years for which the number of frost events remained below (above) the total annual mean during the autumn and winter months.

The presence of clouds traps some of the heat emitted from the earth's surface and reemits back towards the earth, resulting in slower nighttime temperature decrease than under clear sky. On the other hand, Silvestri (2005) shows that the winter precipitation during El Niño phase is significantly greater than in La Niña and neutral cases in the southeast sector of SESA. More recently, Tedeschi et al. (2016) demonstrated that Canonical El Niño produces positive precipitation anomalies and more extreme precipitation events than climatology over SESA in the JJA season. This increase in precipitation and cloudiness could be the reason for the warmer conditions at nights.

3.2.3. *Regional atmospheric circulation*

Indices related to regional atmospheric circulation presented the strongest influence on the JJA TN10 (Fig. 5b). The May blocking index (IB) is significantly correlated with winter cold nights in almost 70% of the stations, while the intensity and latitudinal position of SPA (represented by indices APINT and APLAT) are associated with JJA TN10 in almost half of the stations. The zonal wind at 200 hPa on the northern flank of the subtropical jet (U1) is also important indicating significant correlations in 23% of the stations.

Our results indicate that a higher occurrence of cold nights in northern Argentina is preceded in May by an above normal intensity of the northern flank of the subtropical jet (Fig. 6b). Consistently, previous works found a relationship between the intensification of the subtropical jet in South America and the higher frequency of generalized frosts (Müller et al., 2005, Müller, 2007). According to these studies, a weakening of the subtropical jet around 25 °S favors the occurrence of positive temperature anomalies in the Wet Pampas as this allows a quick passage of frontal systems to the north of 30 °S and the re-establishment of the circulation with a northern component over most of Argentina. More recently, Müller and Berri (2012) specified that generalized frosts persistence depends among other things on the magnitude of the confluence in the jet entrance region in subtropical latitudes; while generalize frosts with intermediate persistence depend on the greater jet acceleration which favors a predominantly meridional Rossby wave train propagation with a confluence region to the west of the continent prior to the event.

The SPA and blocking indices can be considered good predictors of the JJA TN10. Throughout the region of interest, IB is an excellent

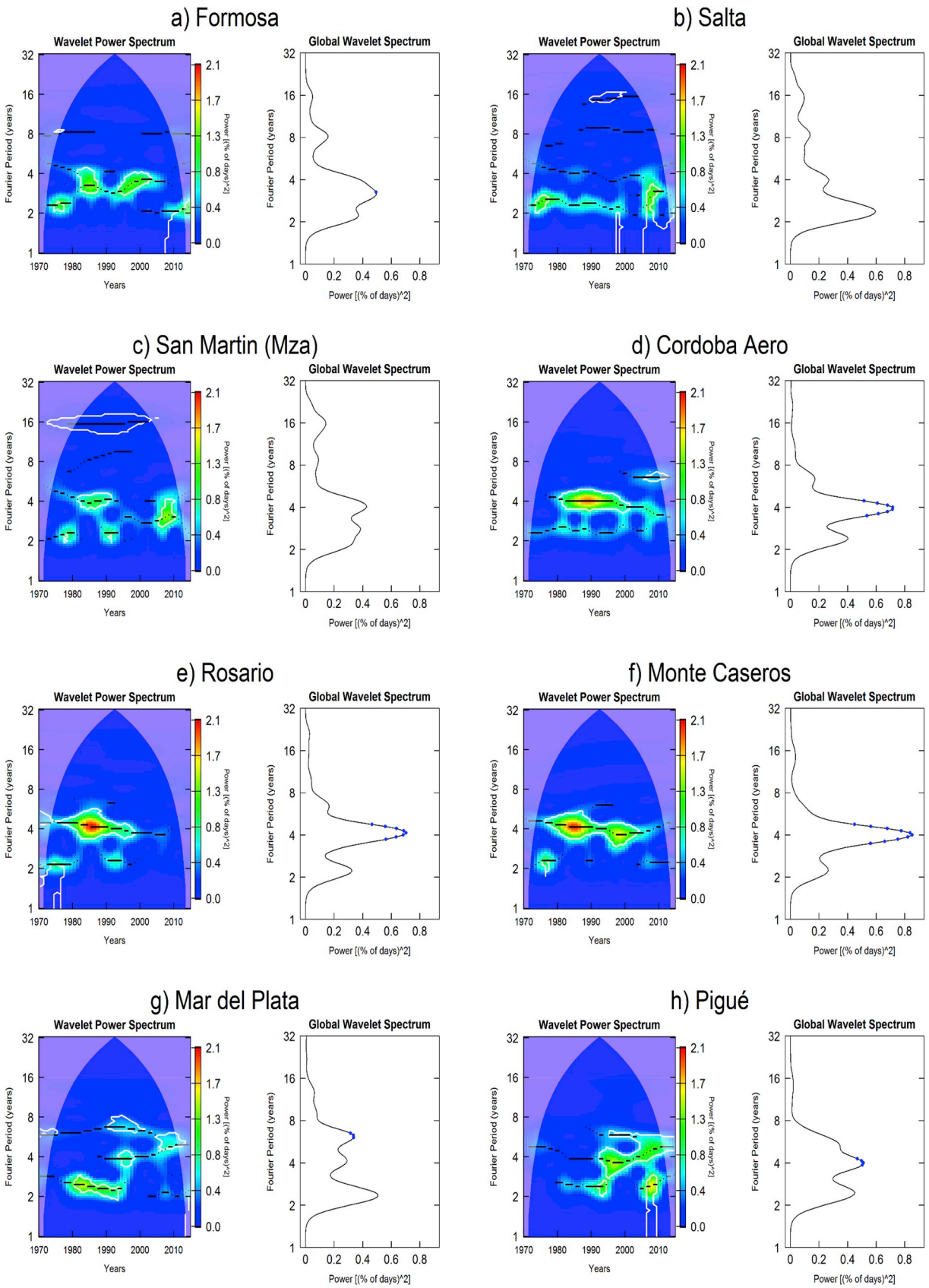

Fig. 3. Wavelet power spectra of JJA TN10 Fourier periods are shown on the vertical axis and the years on the horizontal axis. White contours indicate the significant periods at 10% and the black lines the local maximums of the wavelet transform that provides an estimate of instantaneous periods (left). Average wavelet power (right) shows on the vertical axis the Fourier periods and on the horizontal axis the averages. The points indicate those averages that were significant at 5% contrasting with the spectrum that would be obtained for the white noise.

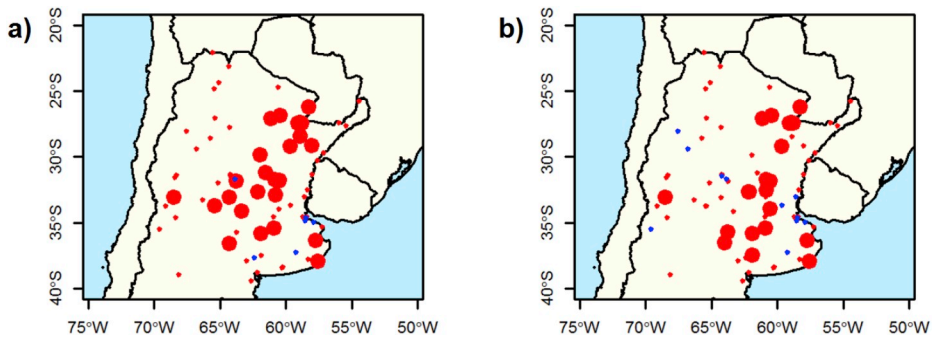

Fig. 4. Correlation between JJA TN10 and May TN10 (a) and MAM TN10 (b). Significant positive correlations at 95% confidence level (big red dots), positive non-significant correlations (small red dots), negative non-significant correlations (small blue dots). (For interpretation of the references to color in this figure legend, the reader is referred to the Web version of this article.)

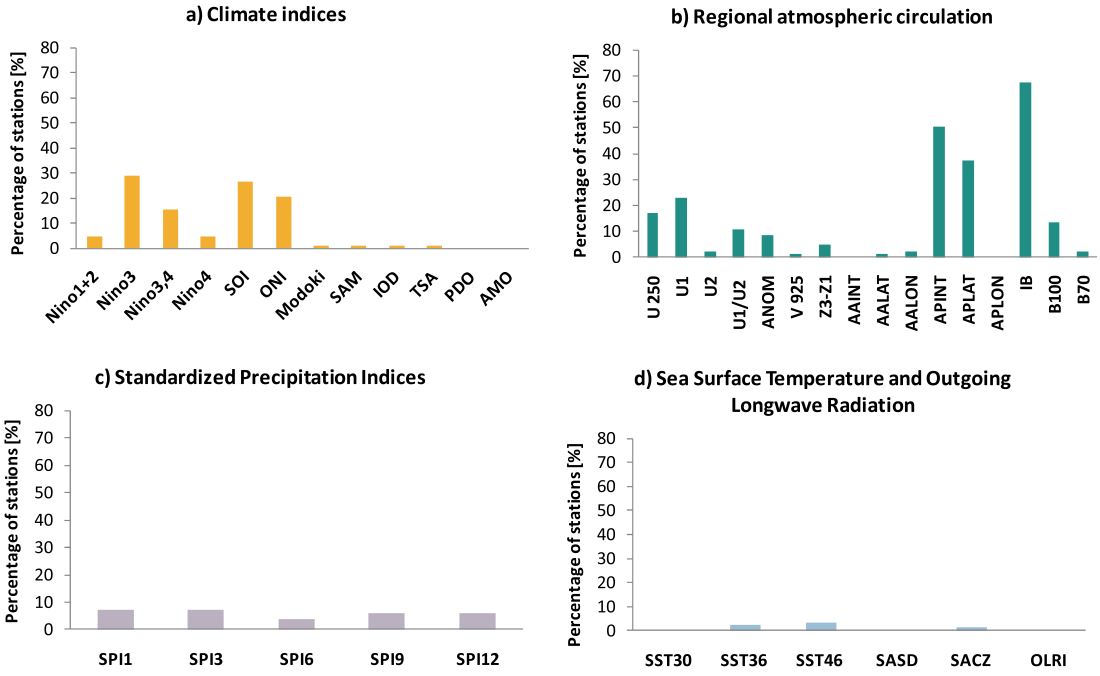

Fig. 5. Percentage of stations significantly correlated at 95% confidence level. The correlations were calculated between the different candidates to predictors in May and subsequent JJA TN10 in the 1970–2015 period. a) Climate indices, b) Regional atmospheric circulation c) Standardized Precipitation Indices d) Sea Surface Temperature and Outgoing Longwave Radiation.

predictor of cold nights: the occurrence of blocking events over the Pacific Ocean (high values of the IB index) in May is associated with a lower frequency of cold extremes of minimum temperature during winter, approximately 5% lower frequency than when IB presents low values (Fig. 6c). These warming conditions of minimum temperature agree with results by Mendes et al. (2008) for the winter mean temperature in the presence of blocking events in the southeastern Pacific. The blocking pattern can generate SST anomalies that could be a precursor for extreme temperature events (Köhl and Vlasenko, 2019). Fig. 7 presents composites of SST and geopotential height anomalies at 500 hPa in winter when the May IB index registered above and below normal values. SST shows an ENSO-like pattern with El Niño (La Niña) like after above (below) normal blocking events (Fig. 7 a-b). Other differences among the SST fields are observed in central South Pacific and on the coast of Argentina and Chile. Warm (cold) SST anomalies are favored after above (below) normal May IB which coincides with a lower (higher) occurrence of cold extremes of the minimum temperature.

On the other hand, after above normal May IB, geopotential height at 500 hPa shows a wave-train that emanates from central Pacific which reaches the Antarctic Peninsula and then is reflected toward South America (Fig. 7 c). A similar pattern of geopotential height, but more intense, can be found when the El Niño3 index presents below normal values (not shown). A wave-train is not observed after below normal May IB (Fig. 7 d).

Previously, it has already been found that the ENSO-like pattern influences the temperature in South America. Barros et al. (2002) found warm (cold) temperature anomalies in subtropical South America during the winter of the developing phase of El Niño (La Niña) due to enhanced (weakened) northerly flow.

The intensification and southward shift of the SPA in May favors an increase in the occurrence of cold extremes of the minimum temperature (Fig. 6d and e). It may possibly be related to more favorable conditions leading to the entrance of post-frontal migratory anticyclones associated with clear sky and calm winds over central Argentina (Garreaud, 2000).

The other indices considered (SPI, Atlantic SST, and South American monsoon) showed few significant correlations with JJA TN10 and are

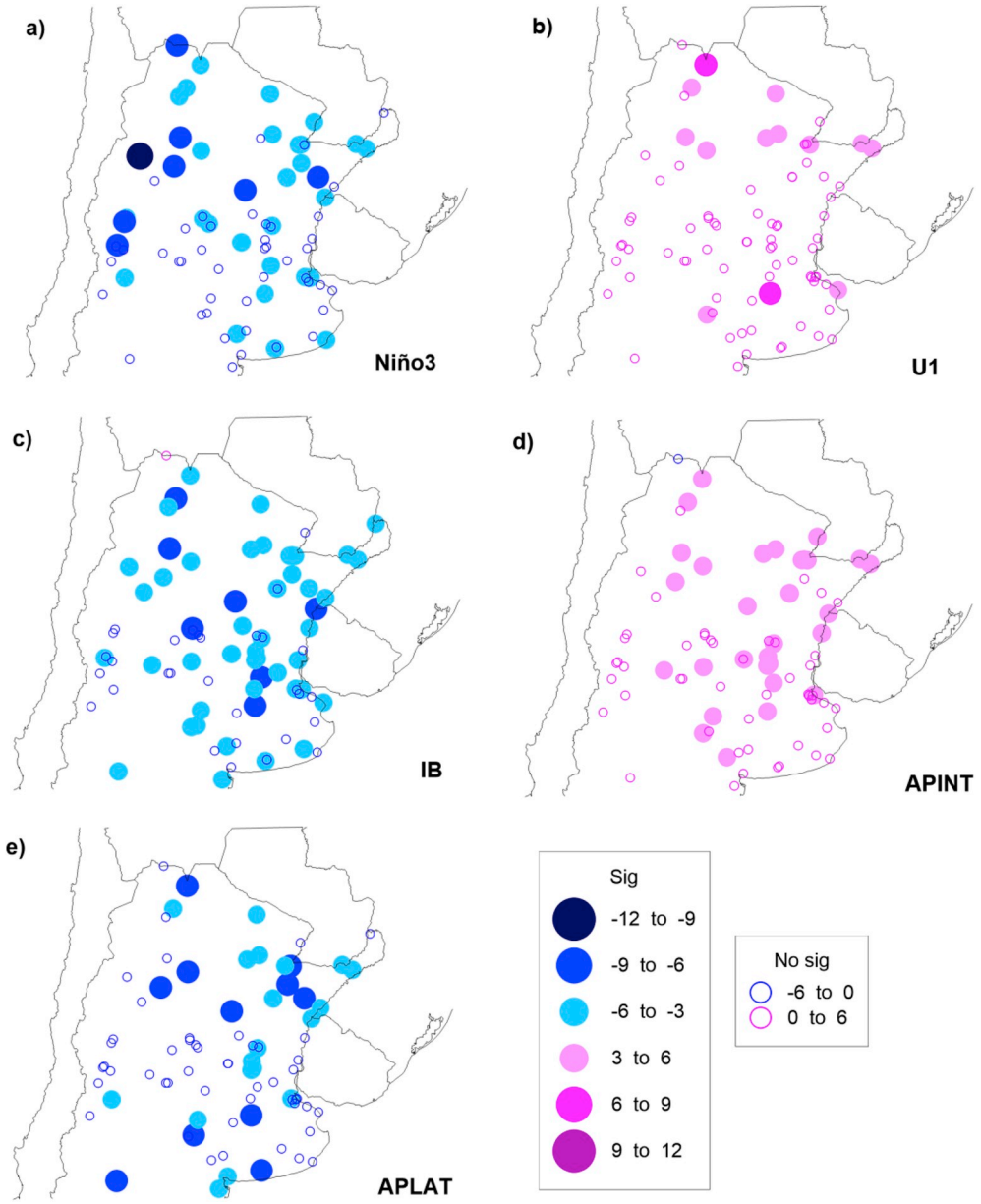

Fig. 6. Difference fields between JJA TN10 for years when the predictors, exceeded the second tercile and the same for years when the index was lower than the first tercile [% of days]. The solid (empty) dots represent significant (not significant) differences with 95% confidence.

not considered as good predictors as those discussed above (Fig. 5c and d).

3.3. Influence of ENSO phase on JJA TN10 and predictors of JJA TN10 under ENSO neutral conditions

In Section 3.2.2, we found that May Niño 3 is a source of predictability for JJA TN10. However, even if the Niño 3 index is above normal in a particular month, it does not imply that El Niño phase is present, since warm anomalies must endure and be above a certain threshold for at least five consecutive months in the equatorial Pacific. In order to obtain a better understanding of the JJA TN10 differences between the three ENSO phases, we analyzed the JJA TN10 distributions for each phase. The ONI index of the previous season (MAM) was used for the phase classification (Table 1). The ONI index was chosen because it is the standard index that NOAA uses for identifying El Niño and La Niña events in the tropical Pacific.

We first clustered the stations into four regions according to JJA TN10 values by using K-means method (Fig. 8), to estimate distributions in each region. Box plots (Fig. 9) show the JJA TN10 distributions for each ENSO phase and region. In all four regions, the median under El Niño phase is lower than under the other phases. Cold extreme events of the minimum temperature in region 1 are more likely to occur if the MAM season is under neutral phase. Additionally, in this region there is not enough evidence to reject the null hypothesis of K–S test at 95% confidence level when comparing JJA TN10 distributions under El Niño and La Niña (i.e. we cannot say that the distributions differ). In regions 2 and 3, under autumn El Niño conditions it is unlikely that the JJA TN10 index will present values higher than 25%, while following La Niña conditions there is always at least one case of cold extreme throughout the winter. The JJA TN10 distributions for La Niña and neutral phases are similar in region 2, while all the distributions are different in region 3. High values of JJA TN10 might occur in region 4 under any of the phases of the ENSO (although they are more likely under neutral conditions); however, that distributions differ significantly from each other. In summary, El Niño conditions during autumn would favor less

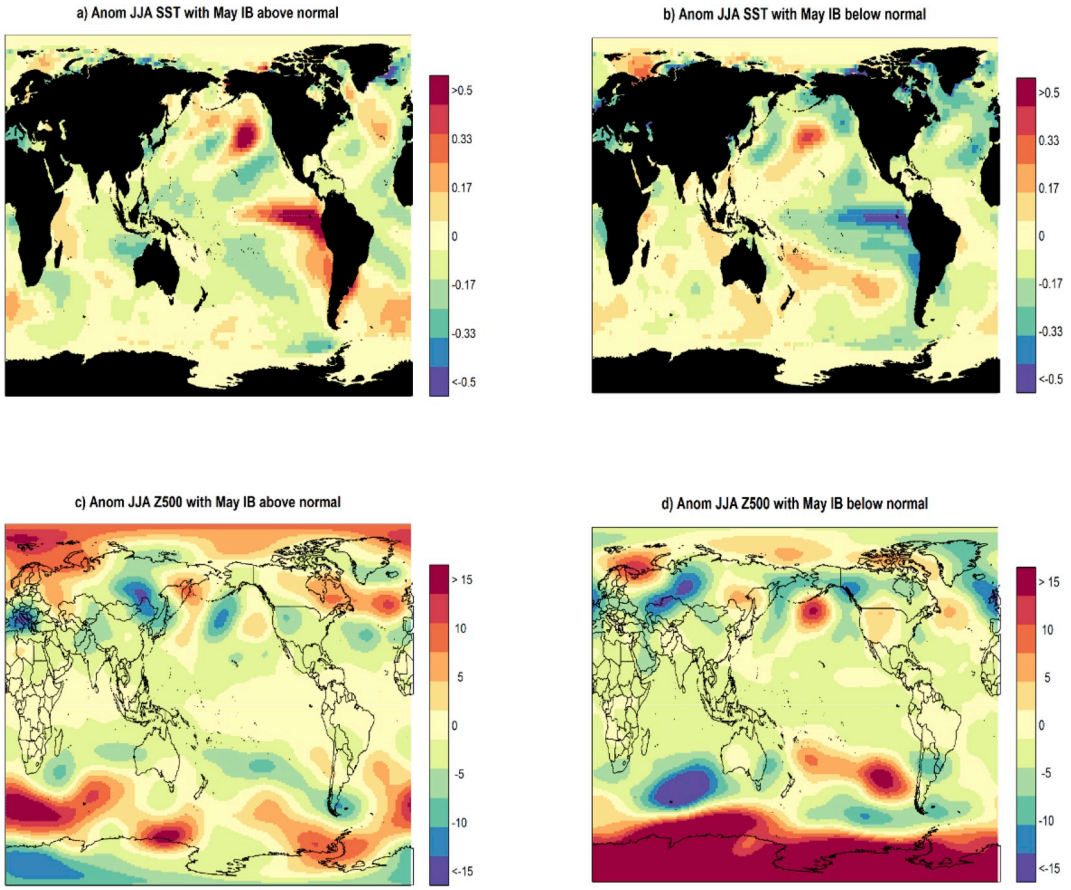

Fig. 7. Composites of the anomaly sea surface temperature from NOAA ERSST V5 (a–b) and geopotential height at 500 hPa from NCEP/NCAR R1 (c–d) when May blocking index presents above and below normal values in the period 1970–2015. Climatology 1981–2010.

Table 1
Classification of the years in ENSO phases according to MAM ONI.

La Niña	Neutral	El Niño
1971, 1974, 1975, 1985, 1989, 1999, 2000, 2008, 2011	1970, 1972, 1973, 1976, 1977, 1978, 1979, 1980, 1981, 1984, 1986, 1988, 1990, 1991, 1993, 1994, 1995, 1996, 1997, 2001, 2002, 2003, 2004, 2006, 2007, 2009, 2012, 2013, 2014	1982, 1983, 1987, 1992, 1998, 2005, 2010, 2015

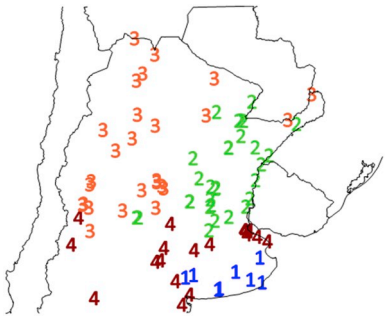

Fig. 8. K-means clusters of stations according to JJA TN10.

frequency of cold extreme events in winter, but not necessarily La Niña conditions would favor a higher frequency. Furthermore, we observed that high values of JJA TN10 are also less likely to occur in the four regions if the El Niño phase is present in the seasons April–June, May–July and JJA (not shown).

In particular, we analyzed the frequency of low occurrence of cold extreme events in winter (JJA TN10 values below to 5%) and high occurrence of cold extreme events (JJA TN10 values above to 20%) considering different ENSO phases in the previous season (not shown). Cases with low frequencies of cold extremes were rare in region 3, and they were mostly preceded by El Niño condition. In the other regions, more cases with low values of JJA TN10 were also preceded by El Niño phase. This was principally seen in regions 2 and 4. The analysis of high frequencies of cold extreme events did not yield differences among ENSO phases as marked as those observed with low frequencies. Winters with high JJA TN10 were more frequently preceded by neutral phases in region 1 and, to a lesser extent, in regions 2 and 4. Finally, slightly more cases with a high occurrence of cold extremes were preceded by La Niña phase in region 3.

Subsequently, since most of the years were classified as neutral and predictability is reduced during this phase (Osman and Vera, 2016), we looked for JJA TN10 predictors specifically under previous ENSO neutral conditions by correlating all the indices with JJA TN10 only in neutral years of ENSO. We observed that the percentage of stations with significant correlations between JJA TN10 and the regional predictors are reduced by almost 35%; nevertheless, IB is still a relevant predictor of winter cold nights (Fig. 10b). Particularly, U1 lost its usefulness as predictor under neutral conditions because it is associated with JJA TN10 at 95% confidence level only in two stations. On the other hand, we detected that SAM index becomes an important predictor under ENSO neutral conditions (Fig. 10a), while the rest of the indices remain of little relevance.

Fig. 11 shows the correlations between JJA TN10 and different climate indices only considering neutral conditions. The SAM index is

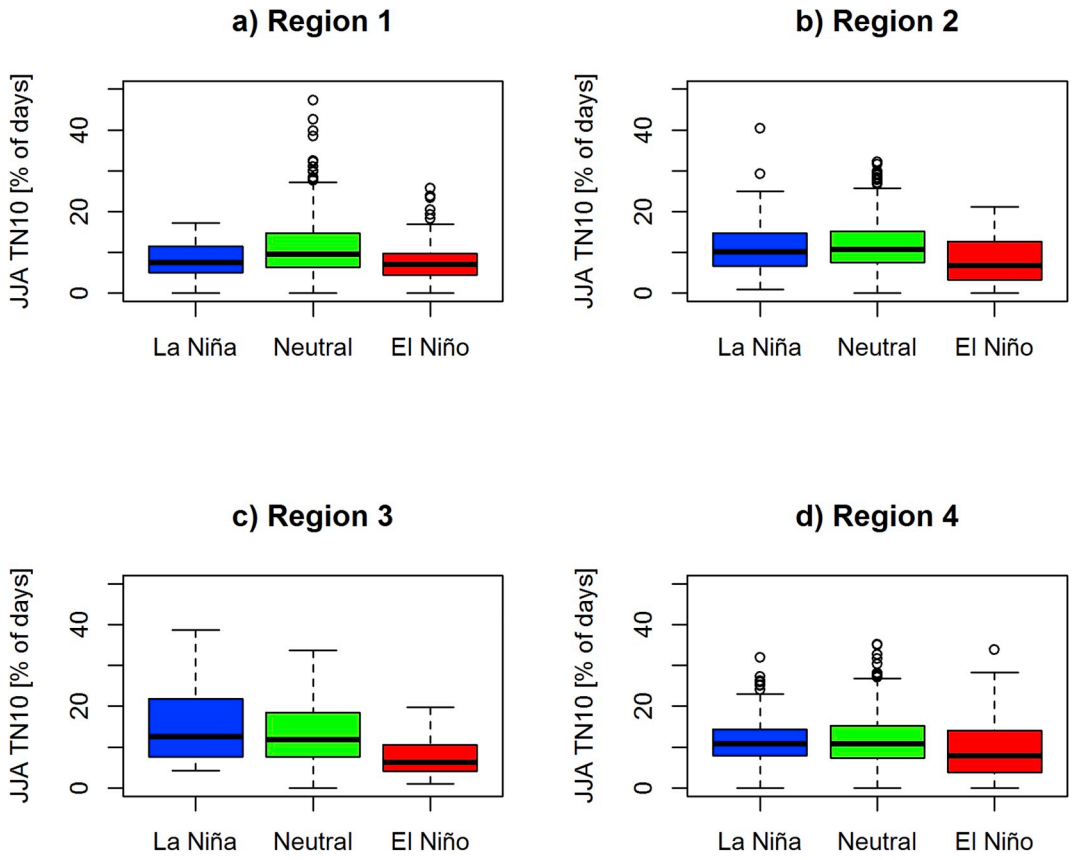

Fig. 9. Boxplots of JJA TN10 for each ENSO phase (classified according to MAM ONI) in each of the regions. The bottom and top of the box are always the 25th and 75th percentile, and the band near the middle of the box is the median. The whiskers extend up to 1.5 times the interquartile range from the top (bottom) of the box to the furthest data within that distance. If there are any data beyond that distance ('outliers'), they are represented individually as points. a) Region 1 in southeast, b) Region 2 in northeast, c) Region 3 in northwest, d) Region 4 in south.

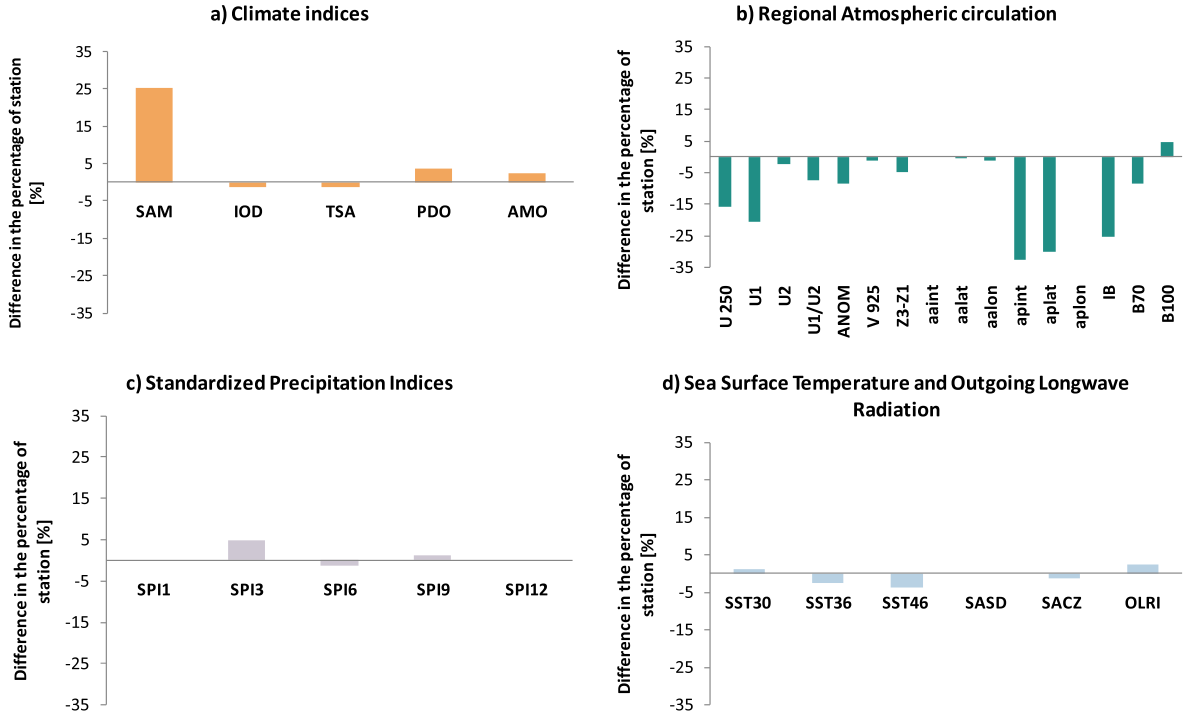

Fig. 10. Difference of the percentage of stations correlated significantly at 5% with the indices when only the ENSO neutral conditions are considered with respect to the percentage with significant correlations previously observed in Fig. 5.

significantly correlated with JJA TN10 in eastern Argentina, where a positive phase of SAM in May favors colder conditions of minimum temperature due to an increase of the occurrence of JJA TN10. A considerable amount of studies demonstrated that SAM has potential influence on the South Hemisphere climate system, affecting sea–air–ice system, sea temperatures, surface heat fluxes, meridional heat fluxes, mixed layer depths, regional rainfall and even oceanic meridional Ekman transport (e.g., Marshall, 2003, 2007; Reason and Rouault, 2005; Gillett et al., 2006; Hendon et al., 2007; Sen Gupta and England, 2007; Harry et al., 2014; Lim and Harry, 2015; Zheng et al., 2015). Since the thermal inertia of the ocean, SST can store the abnormal SAM signal via air–sea interactions and persist it for an extended period than the initial atmospheric signal and then influence the regional climates in the subsequent months (Shukla, 1998; Sen Gupta and England, 2007; Lin and Wu, 2011; Wu et al., 2009a, b, 2014). The May SAM anomalies can indeed lead to SST anomalies in June–July by affecting the surface wind speed (Dou et al., 2017). In particular, Xiao et al. (2016) show that the SAM-induced meridional dipolar sea surface temperature anomalies, through surface heat fluxes, can maintain persistent lower tropospheric temperature anomalies. As the zonal wind shifts poleward in the SAM, a significant meridional dipolar structure SST anomaly, with cold anomalies at high latitude (50°–70°S) and warm anomalies at midlatitude (35°–50°S), emerges at positive lags and lasts for nearly 100 days. The surface air temperature displays broad warm anomalies over the midlatitudes, which is consistent with the positive surface heat flux from the atmosphere to the ocean. In Australia, Marshall et al. (2012) found that when the SAM is strong in the initial conditions, there is higher skill in forecasting rainfall anomalies over eastern Australia and maximum temperature anomalies over most of the continent during June–November at lead times of 2–3 weeks, compared with when the SAM is weak. Moreover, Risbey et al. (2019) found that 10 to 5 days before winter frost events in Australia the geopotential height at 500 hPa show a SAM-like wave structure with highs in each of the ocean basins bounded by lower than average pressure poleward.

Regarding the other predictors, both IB and APINT presented the same sign and spatial distribution of the significant correlation with JJA TN10 than the one previously observed in Fig. 6 c-d, but fewer stations are significantly correlated. In particular, in northwestern Argentina, almost no significant correlation remains with the blocking index.

In general, we observed less influence of the different processes under ENSO neutral conditions, finding only one new useful predictor while those we had previously determined lost influence in certain regions. Therefore, the low number of predictors hinders the seasonal prediction of JJA TN10.

3.4. Case studies: the warmer and cooler winters for the 1970–2015 period

In this section, we analyzed the key meteorological drivers of winter cold nights for the years 1986 and 2007, when several stations presented the lowest and highest values of the JJA TN10 index, respectively. Fig. 12a and b shows the spatial distribution of cold nights during these years. In 1986, JJA TN10 presented a minimum in northeastern Argentina with a percentage of 0% days with cold nights during that winter, which indicates strong warmer conditions of the minimum temperature. A prevalence of positive temperature anomalies in the whole central and northern part of Argentina was already shown by Müller et al. (2005), without generalized frost occurrence for 1986 winter. In contrast, 2007 showed a maximum value of 50% of days with cold nights in the southeastern region. In particular, snow was recorded in Buenos Aires in 2007 for the first time in 90 years. The event was driven by a large high-pressure region just west of southern South America, flanked by two deep lows in the South Pacific and South Atlantic, and the resulting winds generated cold advection toward mid-latitudes (BAMS, 2008; Pezza et al., 2010).

In order to study the associated atmospheric circulation, we employed ERA-Interim monthly data: minimum temperature (TN), sea level pressure (SLP), geopotential height at 500 hPa (GH500), and zonal winds at 200 hPa. We compute anomalies of all variables with respect to the climatological period 1981–2010. Since both cases of studied occurred after 1979, we used ERA-Interim reanalysis. According to Lovino et al. (2018), ERA-Interim can recognize temperature extremes in time and space and it also has a higher resolution than NCEP/NCAR Reanalysis 1. Fig. 12c and d presents TN winter anomalies in 1986 and 2007, respectively. These fields agree with the JJA TN10 fields (Fig. 12a and b) since the maximum and minimum values of the anomalies concur with the extreme values of JJA TN10. The climatological value expected for the TN10 index is 10%, according to its definition, so values of TN10 below (above) this threshold would indicate a lower (higher) occurrence of cold extremes than the climatologically expected.

The circulation fields in May present opposite patterns between 1986 and 2007 (Fig. 13). The anomalous fields of SLP and GH500 reveal an equivalent barotropic structure. Moreover, Fig. 13c is similar to the GH500 composite made by Mendes et al. (2008) for blocking events in the Southeast Pacific, i.e., it shows negative anomalies of GH500 centered at 40°S-110°W and a positive one centered at 65°S-115°W. Therefore, as we mentioned before, the occurrence of blocking events in May weaken the SPA and inhibit the occurrence of winter cold nights. Associated with the blocking events, the westerlies in the northern flank of the subtropical jet are weakened (Fig. 13e). While May precipitation did not show important differences between the two years (not shown), we observed marked differences in the specific humidity anomalies at 850 hPa in JJA between the two cases (Fig. 12e and f). This result indicates that warmer air mass is holding more water vapor than a colder one and the possible occurrence of positive feedback between temperature and water vapor which amplifies the effect of water vapor: an increase of the atmospheric humidity produces an increase of the absorption of long-wave radiation emitted by the surface, which in turn causes a rise in temperature and a warmer atmosphere can contain more water vapor.

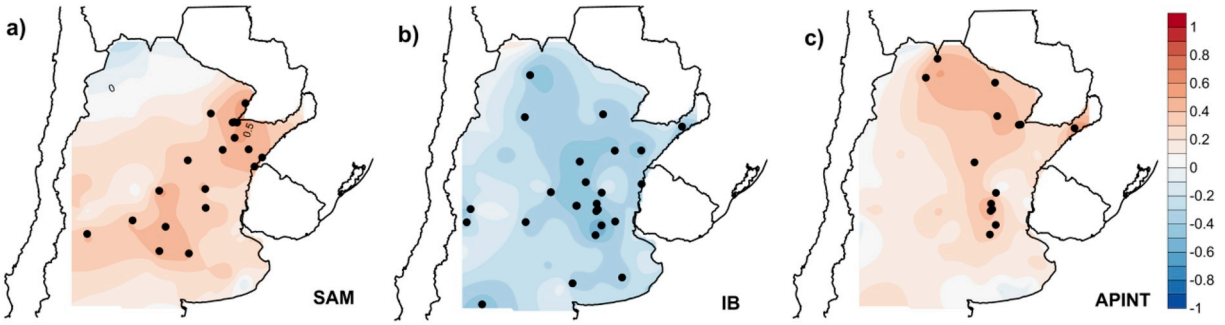

Fig. 11. Correlation between JJA TN10 and SAM (a), IB (b) and APINT (c) in May under ENSO neutral conditions. Dots indicate significant correlations at 95% confidence level.

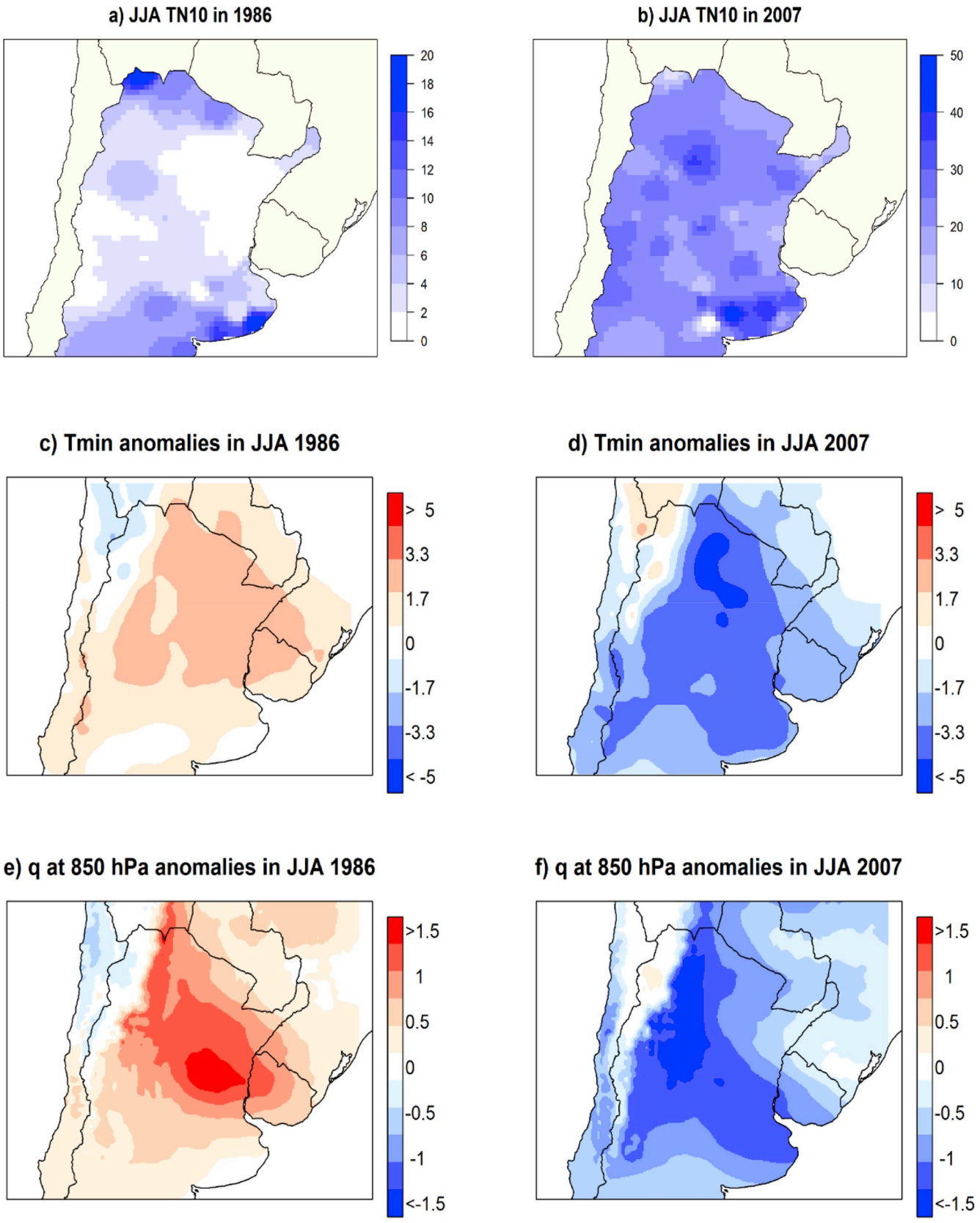

Fig. 12. Winter cold nights (JJA TN10) in 1986 (a) and 2007 (b). Anomalies of minimum temperature in JJA (c and b, °C) and anomalies of specific humidity at 850 hPa in the winter (JJA) of 1986 (e) and 2007 (f) using ERA-Interim reanalysis (g kg^{-1}). Climatology 1981–2010.

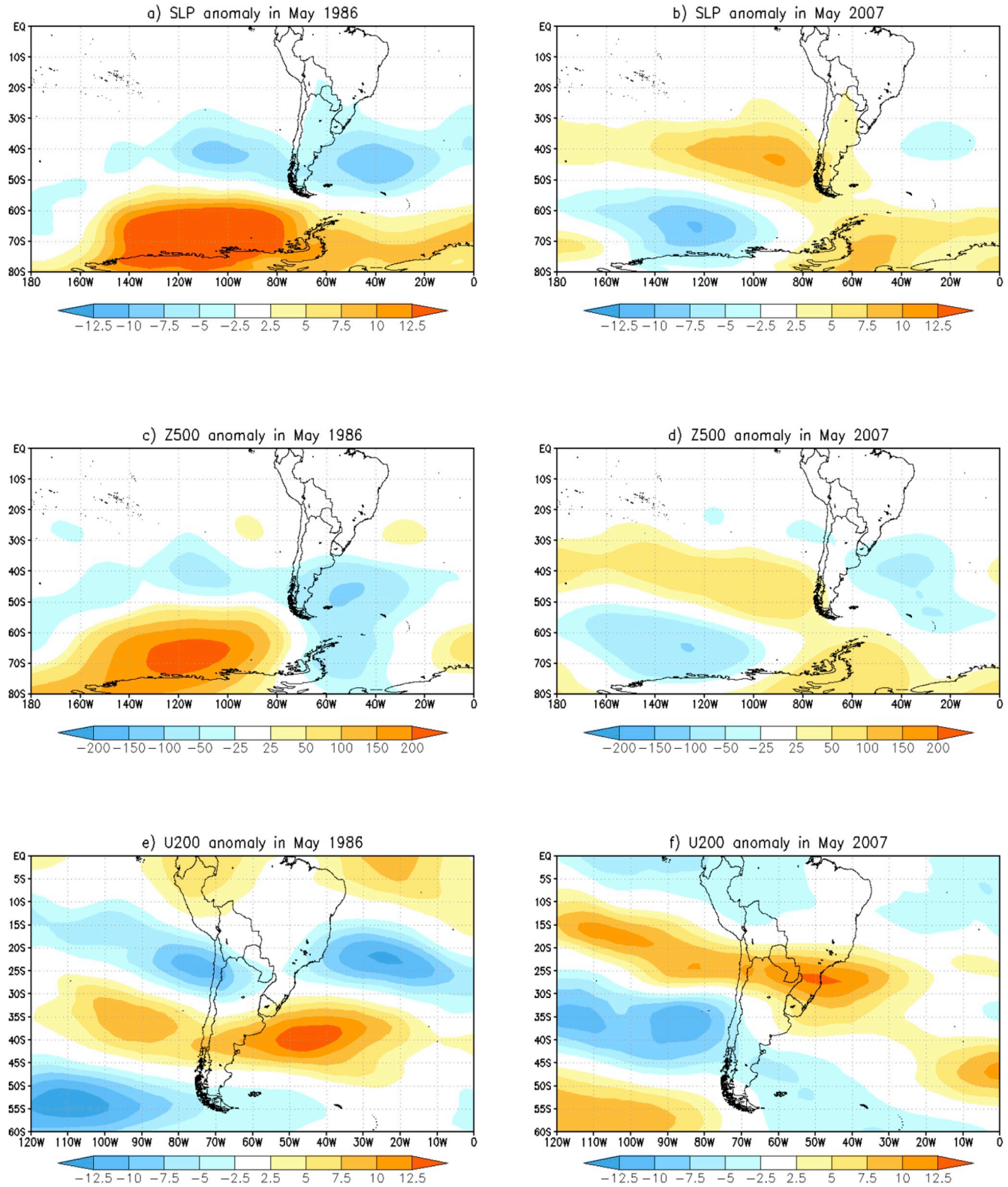

Fig. 13. Anomalies of sea level pressure (a and b, hPa), geopotential height at 500 hPa (c and d, m) and zonal wind at 200 hPa (e and f, m/seg) in May 1986 (left column) and May 2007 (right column) using ERA-Interim reanalysis. Climatology 1981–2010.

Regarding the role of climate indices, both winter seasons occurred after autumn ENSO neutral conditions (based on the ONI index). The SAM index registered negative phases in May for both years. Nevertheless, the persistence of TN10 in eastern Argentina could be considered a useful predictor for both years since May TN10 presented low (high) values in 1986 (2007). Table 2 ranks predictors for those two years, indicating in which tercile predictors were located and how they affect the JJA TN10, based on their correlations. We decided to show the signal of the five main predictors found without discriminating the ENSO phase, plus the SAM index because according to the ONI values

the previous conditions were neutral. Only two predictors (SAM and APINT) contribute in 1986 to a reduction of the number of days with cold extremes of minimum temperature. In contrast, in 2007, all predictors except SAM, favor colder conditions of minimum temperature. The "unexpected" results related to the SAM index in 2007 can be explained by the results presented in Agosta and Barrucand (2012). The authors analyzed the mean conditions of the tropospheric circulation and possible forcing associated with cold (TN10) and warm (TN90) nights during the austral winter (JJA) in Subtropical Argentina. In particular, they found that low TN10 values are linked to a negative phase of the Southern Annular Mode, but an opposite pattern for high TN10 values was not found. Anomalous convection over the monsoon Indian area and the western tropical southern Indian was the principal physical process related in that case. These characteristics observed for the winter season could be related to this case but considering SAM conditions during the previous month. With all predictors indicating extreme cold conditions, SAM would not be a useful index to consider in the winter seasonal forecast, but if there are no signals of these conditions, it may be useful as a predictor of low TN10 values.

Table 2
Terciles in which the predictors are located in the two extreme cases of 1986 and 2007. The colors indicate how these values of the predictors affect TN10: colder conditions of the minimum temperature (blue), neutral conditions (gray), warmer conditions (pink).

	1986	2007
Niño3	2º	1º
SAM	1º	1º
U1	2º	3º
IB	2º	1º
APINT	1º	3º
APLAT	2º	1º

4. Summary and conclusions

This work includes a detailed study of the potential predictors for winter cold nights (JJA TN10) in Argentina north of 40°S, considering the 1970–2015 period. The predictability of an event is the result of many processes and mechanisms acting over a wide range of time scales. Therefore, we analyzed a large number of predictors: global climate indices, regional circulation indices, standard precipitation indices and SST in the nearby ocean.

We detected significant negative trends in the JJA TN10 series, mainly in the western part of the domain; trends were filtered for the rest of the analysis. Wavelet transforms allowed us to distinguish a periodicity of 4 years as the main signal, probably associated with ENSO, but the signal was not continuous during the entire period.

Spearman lag correlation was used to detect predictors for winter cold nights. Among the main predictors, we could mention persistence of TN10, ENSO, northern flank of the subtropical jet, blocking events, intensity and latitudinal position of SPA. In particular, TN10 one month before winter (May) can be considered a predictor of cold nights mainly in eastern Argentina due to the persistence observed in the series. In general, the influence of El Niño on extreme temperature is related with a lower occurrence of cold extreme events of the minimum temperature. On the other hand, blocking events together with a weaker subtropical jet and a less intense SPA with a northward shift can also inhibit the occurrence of cold extremes of the minimum temperature.

The influence of the ENSO on JJA TN10 was studied in detail. El Niño phase during autumn favors a low occurrence of extreme cold events in winter throughout the region. However, we cannot state the opposite about La Niña phase. Depending on the region, the greater frequency of winter cold nights has been preceded, mostly, by autumns in the neutral phase or La Niña phase. Moreover, during the period analyzed, there were many cases of high frequencies of cold extremes under ENSO neutral conditions, so we analyzed predictability and searched for predictors under ENSO neutral conditions. We observed that the SAM index is a new predictor under this condition in eastern Argentina while the previously found predictors lost influence on JJA TN10 in certain regions.

Finally, we studied the atmospheric circulation associated with two extreme winters with a high and low frequency of cold nights. In both cases, we detect the presence of an equivalent barotropic structure located in the southeastern Pacific in the previous month but with opposite patterns: a cyclonic (anticyclonic) anomaly at 40°S and an anticyclonic (cyclonic) anomaly at 65°S in 1986 (2007). We also found opposite patterns of zonal winds at 200 hPa and column water vapor. All predictors (except for SAM) contributed to colder minimum temperatures in 2007, one of the coldest winters in recent memory. In the case of the warm winter in 1986, which occurred under ENSO neutral conditions, SAM and APINT were useful as predictors. Considering that the SAM modulates the low frequency of cold nights, it would not be an adequate predictor for TN10 when there are strong indications of very cold conditions for the winter (as was the case in 2007), but it would be a useful predictor when there are no signals indicating such conditions.

In this study we looked for predictors of an extreme temperature index (cold nights frequency, commonly known as TN10) on a seasonal scale (winter). In the future, this analysis will be extended to other extreme temperature indices and seasons, in order to create a probabilistic forecast. Considering previous studies and given the results presented here, we will fit statistical models for all years and only for ENSO neutral conditions.

Acknowledgements

This research was supported by CONICET PIP 0137-Res 4248/16 from National Council of Scientific and Technical Research, Argentina and UBACyT 2018 20020170100357BA from University of Buenos Aires, Argentina. We want to thank the National Weather Service of Argentina and National Institute of Agricultural Technology for providing the data for this study. The authors want to thank Dr. Graciela Raga for her collaboration.

Appendix A. Supplementary data

Supplementary data to this article can be found online at https://doi.org/10.1016/j.wace.2019.100236.

References

Agosta, E.A., Barrucand, M.G., 2012. Mean winter conditions and quasi-stationary rossby waves associated with the winter frequency of warm and cold nights in subtropical Argentina. Geoacta 37 (2), 147–166. ISSN 1852-7744.

Alessandro, A.P., 2014. Incidence and trend of blocking action situations on the temperature and precipitation in Argentina. Atmósfera 27 (2), 141–163. https://doi.org/10.1016/S0187-6236(14)71106-3.

Ashok, K., Behera, S.K., Rao, S.A., Weng, H., Yamagata, T., 2007. El nino Modoki and its possible teleconnection. J. Geophys. Res. 112 https://doi.org/10.1029/2006JC003798. C11007.

BAMS, 2008. State of climate in 2007. In: Levindon, D.H., Lawrimore, J.H. (Eds.), Special Supplement to the Bulletin of the American Meteorological Society. Vol. 89, No. 7, July 2008.

Barlow, K.M., Christy, B.P., O'Leary, G.J., Riffkin, P.A., Nuttall, J.G., 2015. Simulating the impact of extreme heat and frost events on wheat crop production: a review. Field Crop. Res. 171, 109–119. https://doi.org/10.1016/j.fcr.2014.11.010.

Barros, V., Grimm, A., Doyle, M., 2002. Relationship between temperature and circulation in southeastern South America and its influence from El nino and La nina events. J. Meteorol. Soc. Jpn. 80 (1), 21–32.

Barrucand, M., Rusticucci, M., Vargas, W., 2008. Temperature extremes in the South of south America in relation to atlantic ocean surface temperature and southern

Hemisphere circulation. J. Geophys. Res. Atmos. 113 https://doi.org/10.1029/2007JD009026. D20111.
Best, D., Roberts, D., 1975. Algorithm AS 91: the percentage points of the χ2 distribution. J. R. Stat. Soc. Ser. C (Appl. Stat.) 24 (3), 385–388. https://doi.org/10.2307/2347113.
Cerne, B., Vera, C.S., 2011. Influence of the intraseasonal variability on heat waves in subtropical South America. Clim. Dyn. 36, 2265. https://doi.org/10.1007/s00382-010-0812-4.
Collazo, S., Barrucand, M., Rusticucci, M., 2019. Summer seasonal predictability of warm days in Argentina: statistical model approach. Theor. Appl. Climatol. https://doi.org/10.1007/s00704-019-02933-6.
Dou, J., Wu, Z., Zhou, Y., 2017. Potential impact of the May Southern Hemisphere annular mode on the Indian summer monsoon rainfall. Clim. Dyn. 49, 1257. https://doi.org/10.1007/s00382-016-3380-4.
Enfield, D.B., Mestas, A.M., Mayer, D.A., Cid-Serrano, L., 1999. How ubiquitous is the dipole relationship in tropical Atlantic sea surface temperatures? J. Geophys. Res. Oceans 104, 7841–7848. https://doi.org/10.1029/1998JC900109.
Enfield, D.B., Mestas-Nunez, A.M., Trimble, P.J., 2001. The Atlantic Multidecadal Oscillation and its relationship to rainfall and river flows in the continental. U.S. Geophys. Res. Lett. 28, 2077–2080.
Foufoula-Georgiou, E., Kumar, P., 1995. Wavelets in Geophysics. Academic Press, 373 pp.
Gallego, D., Ribera, P., García-Herrera, R., Hernández, E., Gimeno, L., 2005. A new look for the southern Hemisphere jet stream. Clim. Dyn. 24 (6), 607–621.
Garreaud, R.D., 2000. Cold air incursions over subtropical South America: mean structure and dynamics. Mon. Weather Rev. 128, 2544–2559. https://doi.org/10.1175/1520-0493(2000)128<2544:CAIOSS>2.0.CO;2.
Gillett, N.P., Kell, T.D., Jones, P.D., 2006. Regional climate impacts of the southern annular mode. Geophys. Res. Lett. 33 https://doi.org/10.1029/2006GL027721. L23704.
Gong, D., Wang, S., 1999. Definition of antarctic oscillation index. Geophys. Res. Lett. 26, 459–462.
González, M.H., Garbarini, E., Romero, P., 2015. Rainfall patterns and the relation to atmospheric circulation in northern Patagonia (Argentina). Adv. Environ. Res. 41, 85–100.
González, M.H., Garbarini, E., Rolla, A.L., Eslamian, S., 2016. Meteorological drought indices: rainfall prediction in Argentina. In: Handbook of Drought and Water Scarcity. Vol. 1, Principle of Drought and Water Scarcity, Chapter 29, 540-567, Taylor & Francis Publishing (CRC Group). Reino Unido, Abingdon, 9781498731089 1498731082, Saeid Eslamian.
Grimm, A.M., Tedeschi, R.G., 2009. ENSO and extreme rainfall events in south America. J. Clim. 22, 1589–1609. https://doi.org/10.1175/2008JCLI2429.1.
Grinsted, A., Moore, J.C., Jevrejeva, S., 2004. Application of the cross wavelet transform and wavelet coherence to geophysical time series. Nonlinear Process Geophys. 11, 561–566. https://doi.org/10.5194/npg-11-561-2004.
Harry, H.H., Lim, E.P., Nguyen, H., 2014. Seasonal variations of subtropical precipitation associated with the Southern Annular Mode. J. Clim. 27, 3446–3460. https://doi.org/10.1175/JCLI-D-13-00550.1.
Hartigan, J.A., Wong, M.A., 1979. Algorithm AS 136: a K-means clustering algorithm. J. Appl. Stat. 28, 100–108. https://doi.org/10.2307/2346830.
Hendon, H.H., Thompson, D.W., Wheeler, M.C., 2007. Australian rainfall and surface temperature variations associated with the Southern Hemisphere annular mode. J. Clim. 20, 2452–2467. https://doi.org/10.1175/JCLI4134.1.
IPCC, 2013. In: Stocker, T.F., Qin, D., Plattner, G.-K., Tignor, M., Allen, S.K., Boschung, J., Nauels, A., Xia, Y., Bex, V., Midgley, P.M. (Eds.), Climate Change 2013: the Physical Science Basis. Contribution of Working Group I to the Fifth Assessment Report of the Intergovernmental Panel on Climate Change. Cambridge University Press, Cambridge, United Kingdom and New York, NY, USA, p. 1535. https://doi.org/10.1017/CBO9781107415324.
James, G., Witten, D., Hastie, T., Tibshirani, R., 2013. An Introduction to Statistical Learning: with Applications in R, Corrected edition. Springer, New York.
Kalnay, E., Kanamitsu, M., Kistler, R., Collins, W., Deaven, D., Gandin, L., Iredell, M., Saha, S., White, G., Woollen, J., Zhu, Y., Chelliah, M., Ebisuzaki, W., Higgins, W., Janowiak, J., Mo, K.C., Ropelewski, C., Wang, J., Leetmaa, A., Reynolds, R., Jenne, R., Joseph, D., 1996. The NCEP/NCAR 40-year reanalysis project. Bull. Am. Meteorol. Soc. 77, 437–472. https://doi.org/10.1175/1520-0477(1996)077<0437:TNYRP>2.0.CO;2.
Kendall, M.G., 1975. Rank Correlation Methods, fourth ed. Charles Griffin, London.
Köhl, A., Vlasenko, A., 2019. Seasonal prediction of northern European winter air temperatures from SST anomalies based on sensitivity estimates. Geophys. Res. Lett. 46, 6109–6117. https://doi.org/10.1029/2018GL081800.
Lim, E.P., Harry, H.H., 2015. Understanding and predicting the strong Southern Annular Mode and its impact on the record wet east Australian spring 2010. Clim. Dyn. 44, 2807–2824. https://doi.org/10.1007/s00382-014-2400-5.
Lin, H., Wu, Z., 2011. Contribution of the autumn Tibetan Plateau snow cover to seasonal prediction of North American winter temperature. J. Clim. 24, 2801–2813. https://doi.org/10.1175/2010JCLI3889.1.
Loikith, P.C., Detzer, J., Mechoso, C.R., Lee, H., Barkhordarian, A., 2017. The influence of recurrent modes of climate variability on the occurrence of monthly temperature extremes over South America. J. Geophys. Res. Atmos. 122 (10) https://doi.org/10.1002/2017JD027561, 297–10,311.
Lovino, M.A., Muller, O.V., Berbery, E.H., Muller, G.V., 2018. How have daily climate extremes changed in the recent past over northeastern Argentina? Glob. Planet. Chang. 168, 78–97. https://doi.org/10.1016/j.gloplacha.2018.06.008.
MacQueen, J., 1967. Some methods for classification and analysis of multivariate observations. In: Proc. Fifth Berkeley Symp. On Mathematical Statistical and Probability. . University of California Press, Berkeley, C.A, pp. 281–297.
Mann, H.B., 1945. Non-parametric tests against trend. Econometrica 13, 163–171.
Mantua, N.J., Hare, S.R., Zhang, Y., Wallace, J.M., Francis, R.C., 1997. A pacific interdecadal climate oscillation with impacts on salmon production*. Bull. Am. Meteorol. Soc. 78, 1069–1080. https://doi.org/10.1175/1520-0477(1997)078<1069:APICOW>2.0.CO;2.
Marshall, G., 2003. Trends in the southern annular mode from observations and reanalyses. J. Clim. 16, 4134–4143. https://doi.org/10.1175/1520- 0442(2003)0162.0.CO;2.
Marshall, G.J., 2007. Half-century seasonal relationships between the southern annular mode and antarctic temperatures. Int. J. Climatol. 27, 373–383. https://doi.org/10.1002/joc.1407.
Marshall, A.G., Hudson, D., Wheeler, M.C., Hendon, H.H., Alves, O., 2012. Simulation and prediction of the Southern Annular Mode and its influence on Australian intra-seasonal climate in POAMA. Clim. Dyn. 38, 2483. https://doi.org/10.1007/s00382-011-1140-z.
McKee, T.B., Doesken, N.J., Kleist, J., 1993. The relationship of drought frequency and duration to time scale. In: Proceedings of the Eighth Conference on Applied Climatology, Anaheim, California, 17–22 January 1993. American Meteorological Society, Boston, pp. 179–184.
McKee, T.B., Doesken, N.J., Kleist, J., 1995. Drought monitoring with multiple time scales. In: Ninth Conference on Applied Climatology. American Meteorological Society, Dallas TX, pp. 233–236. Jan 15-20, 1995.
McLeod, A.I., 2011. Kendall: Kendall rank correlation and Mann-Kendall trend test. R package version 2.2. https://CRAN.R-project.org/package=Kendall.
Mendes, M.C.D., Trigo, R.M., Cavalcanti, I.F.A., Da Camara, C.C., 2008. Blocking episodes in the southern Hemisphere: impact on the climate of adjacent continental areas. Pure Appl. Geophys. 165, 1941–1962. https://doi.org/10.1007/s00024-008-0409-4.
Mueller, B., Seneviratne, S.I., 2012. Hot days induced by precipitation deficits at the global scale. Proc. Natl. Acad. Sci. 109 (31), 12398–12403. https://doi.org/10.1073/pnas.1204330109.
Müller, G.V., 2007. Patterns leading to extreme events in Argentina: partial and generalized frosts. Int. J. Climatol. 27, 1373–1387. https://doi.org/10.1002/joc.1471.
Müller, G.V., 2010. Temperature decrease in the extratropics of South America in response to a tropical forcing during the austral winter. Ann. Geophys. 28, 1–9. https://doi.org/10.5194/angeo-28-1-2010.
Müller, G.V., Berri, G.J., 2012. Atmospheric circulation associated with extreme generalized frosts persistence in central-southern South America. Clim. Dyn. 38 (2012), 837–857. https://doi.org/10.1007/s00382-011-1113-2.
Müller, G.V., Nuñez, M.N., Seluchi, M.E., 2000. Relationship between ENSO cycles and frost events within the Pampa Húmeda region. Int. J. Climatol. 20, 1619–1637. https://doi.org/10.1002/1097-0088(20001115)20:13<1619::AID-JOC552>3.0.
Müller, G.V., Ambrizzi, T., Núñez, M.N., 2005. Mean atmospheric circulation leading to generalized frosts in Central Southern South America. Theor. Appl. Climatol. 82, 95–112. https://doi.org/10.1007/s00704-004-0107-y.
Osman, M., Vera, C.S., 2016. Climate predictability and prediction skill on seasonal time scales over South America from CHFP models. Clim. Dyn. 49 (7–8), 2365–2383. https://doi.org/10.1007/s00382-016-3444-5.
Pezza, A.B., Simmonds, I., Coelho, C.A.S., 2010. The unusual Buenos Aires snowfall of july 2007. Atmos. Sci. Lett. 11, 249–254. https://doi.org/10.1002/asl.283.
Reason, C., Rouault, M., 2005. Links between the Antarctic Oscillation and winter rainfall over western South Africa. Geophys. Res. Lett. 32 https://doi.org/10.1029/2005GL022419. L07705.
Richman, M.B., Leslie, L.M., 2014. Attribution and prediction of maximum temperature extremes in SE Australia. Procedia Comput. Sci. 36, 612–617. https://doi.org/10.1016/j.procs.2014.09.063.
Risbey, J.S., Monselesan, D.P., O'Kane, T.J., Tozer, C.R., Pook, M.J., Hayman, P.T., 2019. Synoptic and large-scale determinants of extreme austral frost events. J. Appl. Meteor. Climatol. 58, 1103–1124. https://doi.org/10.1175/JAMC-D-18-0141.1.
Roesch, A., Schmidbauer, H., 2014. WaveletComp: computational wavelet analysis. R package version 1.0. https://CRAN.R-project.org/package=WaveletComp.
Rusticucci, M., Vargas, W., 2002. Cold and warm events over Argentina and their relationship with the ENSO phases: risk evaluation analysis. Int. J. Climatol. 22, 467–483. https://doi.org/10.1002/joc.743.
Rusticucci, M., Barrucand, M., Collazo, S., 2017. Temperature extremes in the Argentina central region and their monthly relationship with the mean circulation and ENSO phases. Int. J. Climatol. 37, 3003–3017. https://doi.org/10.1002/joc.4895.
Rutllant, J., Aceituno, P., 1991. Southern Hemisphere circulation signals in connection with winter rainfall forecasting in Central Chile. In: Int. Centre for Theoretical Physics, Trieste, Italy. Internal Report IC/91/64: 20 pp.
Saji, N.H., Goswami, B.N., Vinayachandran, P.N., Yamagata, T., 1999. A dipole mode in the tropical Indian ocean. Nature 401 (23), 360–363.
Sen Gupta, A., England, M.H., 2007. Coupled ocean-atmosphere feedback in the southern annular mode. J. Clim. 20 (14), 3677–3692. https://doi.org/10.1175/JCLI4200.1.
Shukla, J., 1998. Predictability in the midst of chaos: a scientific basis for climate forecasting. Science 282, 728–731.
Silvestri, G.E., 2005. Comparison between winter precipitation in southeastern South America during each ENSO phase. Geophys. Res. Lett. 32 https://doi.org/10.1029/2004GL021749. L05709.
Silvestri, G.E., Vera, C.S., 2003. Antarctic Oscillation signal on precipitation anomalies over southeastern South America. Geophys. Res. Lett. 30 (21), 2115. https://doi.org/10.1029/2003GL018277.

Smirnov, N.V., 1939. Estimate of deviation between empirical distribution functions in two independent samples. (Russian). Bull. Moscow Univ. 2 (2), 3–16 (6.1, 6.2).
Tedeschi, R.G., Grimm, A.M., Cavalcanti, I.F.A., 2016. Influence of Central and East ENSO on precipitation and its extreme events in South America during austral autumn and winter. Int. J. Climatol. 36 (15), 4797–4814. https://doi.org/10.1002/joc.4670.
Thompson, D.W., Wallace, J.M., 2000. Annular modes in the extratropical circulation. Part I: month-to-month variability. J. Clim. 13, 1000–1016. https://doi.org/10.1175/1520-0442(2000)013<1000:AMITEC>2.0.CO;2.
Torrence, C., Compo, G.P., 1998. A practical guide to wavelet analysis. Bull. Am. Meteorol. Soc. 79, 61–78. https://doi.org/10.1175/1520-0477(1998)079<0061:APGTWA>2.0.CO;2.
Vera, C.S., Vigliarolo, P.K., 2000. A diagnostic study of cold-air outbreaks over south America. Mon. Wea. Rev. 128, 3–24. https://doi.org/10.1175/1520-0493(2000)128<0003:ADSOCA>2.0.CO;2.
Verdes, P.F., Granitto, P.M., Navone, H.D., Ceccatto, H.A., 2000. Frost prediction with machine learning techniques. In: Proc., VI Argentine Congress on Computer Science, pp. 1423–1433. http://sedici.unlp.edu.ar/bitstream/handle/10915/23444/Documento_completo.pdf?sequence=1.
Wainer, I., Prado, L.F., Khodri, M., Otto-Bliesner, B., 2014. Reconstruction of the South Atlantic Subtropical Dipole index for the past 12000 years from surface temperature proxy. Sci. Rep. 4, 5291. https://doi.org/10.1038/srep05291.
Wilcoxon, F., 1945. Individual comparisons by ranking methods. Biometrics 1, 80–83.
Wilks, D.F., 2006. Statistical Methods in the Atmospheric Sciences, second ed. Academic Press. 627 pp.
Wu, Z.W., Li, J., Wang, B., Liu, X., 2009. Can the Southern Hemisphere annular mode affect China winter monsoon? J. Geophys. Res. 114 https://doi.org/10.1029/2008JD011501. D11107.
Wu, Z.W., Wang, B., Li, J., Jin, F.F., 2009. An empirical seasonal prediction model of the East Asian summer monsoon using ENSO and NAO. J. Geophys. Res. 114 https://doi.org/10.1029/2009JD011733. D18120.
Wu, Z.W., Dou, J., Lin, H., 2014. Potential influence of the November–December Southern Hemisphere annular mode on the East Asian winter precipitation: a new mechanism. Clim. Dyn. 44, 1215–1226. https://doi.org/10.1007/s00382-014-2241-2.
Xiao, B., Zhang, Y., Yang, X.-Q., Nie, Y., 2016. On the role of extratropical air-sea interaction in the persistence of the Southern Annular Mode. Geophys. Res. Lett. 43, 8806–8814. https://doi.org/10.1002/2016GL070255.
Zhang, Y., Wallace, J.M., Battisti, D.S., 1997. ENSO-like interdecadal variability. J. Clim. 10, 1004–1020.
Zheng, F., Li, J., Feng, J., Li, Y., Li, Y., 2015. Relative importance of the austral summer and autumn SAM in modulating southern Hemisphere extratropical autumn SST. J. Clim. 28, 8003–8020. https://doi.org/10.1175/JCLI-D-15-0170.1.